



This is the accepted manuscript made available via CHORUS. The article has been published as:

Searching for spurious solar and sky lines in the Fermi-LAT spectrum

Daniel Whiteson

Phys. Rev. D **88**, 023530 — Published 24 July 2013

DOI: [10.1103/PhysRevD.88.023530](https://doi.org/10.1103/PhysRevD.88.023530)

Searching for Spurious Solar and Sky Lines in the Fermi-LAT Spectrum

Daniel Whiteson¹

¹*Department of Physics and Astronomy, University of California, Irvine, CA 92697*

We search for a unified instrumental explanation of the spectral features seen near $E_\gamma = 130$ GeV in photons collected by Fermi-LAT from the galactic center and from the Earth's limb. We report for the first time a similar feature in photons originating from the vicinity of the Sun, and examine the instrumental characteristics of this Solar feature. To test an instrumental hypothesis, we identify the range of photon incident angles where most of the peak photons are observed in these three spectral features. An examination of the spectrum of photons from the rest of the sky in this angular region reveals a hint of a spectral feature near $E_\gamma = 130$ GeV. These results cast further doubt on the dark-matter-annihilation interpretation of the galactic center peak.

I. INTRODUCTION

The particle nature of dark matter remains a mystery. One potential avenue for discovery is via dark matter annihilation into standard model particles. If the annihilation results in fermions or heavy bosons, photons may be produced via hadronization and the decay of π^0 particles. These photons are expected to be fairly low-energy ($E_\gamma \lesssim 50$ GeV) and are expected to be difficult to distinguish from other sources. A clearer feature may appear from annihilation directly into two-body final states including a photon. Rather than yielding a broad energy spectrum, this process would produce a photon with a well-defined energy simply related to the mass of the dark matter particle. Such high-energy gamma rays typically do not scatter in transit to the Earth from the regions of high dark-matter density where they are produced, making their energy and direction useful handles. The Fermi Large Area Telescope (LAT) has a large field-of-view and excellent energy resolution over a broad range of energy (20 MeV - 1 TeV) [1], making it a powerful probe for peaks in the photon spectrum from dark matter annihilation[2, 3].

Recently, a statistically significant peak has been reported in the Fermi-LAT photon spectrum near $E_\gamma = 130$ GeV[4, 5] with a source close to the galactic center [4–8]. The importance of such a discovery, if interpreted as due to dark matter annihilation, requires a careful exploration of other more mundane explanations, such as potential astrophysical spectral features in the non-dark-matter background from the galactic center, or instrumental effects in the Fermi-LAT detector. Suspicious features have been reported in the incident angle of the photons from the galactic center [9] and a statistically significant feature has been reported in photons from the Earth's limb [10], where no signal is expected from dark matter annihilation.

In this paper, we consider another luminous source, the Sun, for evidence of spectral features. In addition, we use the SPLOTS [11] algorithm to reconstruct – separately for peak and background photons – the distributions of instrumental quantities in an attempt to iden-

tify a common instrumental characteristic unique to the observed spectral features. Such a common characteristic would point strongly to an instrumental explanation which would be independent of the source of the photons. To test such potential instrumental explanations, we examine the spectrum of photons with these instrumental characteristics from the entire sky for evidence of spurious features.

II. THE FERMI-LAT DATA SAMPLE

We use the publically available Fermi-LAT photon data through January 3rd 2013, making standard quality requirements [12, 13]. In addition, we consider several additional requirements for the distinct samples. The analysis of the Earth's limb photons requires a zenith angle (measured with respect to the zenith line, which passed through the earth and the Fermi spacecraft) between 110° and 114° degrees; the analysis of the Solar photons requires a zenith angle less than 105° , rocking angle of less than 52° , and angular distance from the position of the Sun of less than five degrees. The galactic center spectrum is drawn from a five-degree circle around ($l = 0, b = 0$) in galactic coordinates, requiring zenith angle less than 105° and rocking angle of less than 52° .

Other than the reconstructed energy, the photons have other measured characteristics [14] which may give insight into instrumental effects:

- incident angle θ , measured with respect to the top-face normal of the LAT,
- azimuth angle ϕ , measured around to the top-face normal of the LAT such that $\phi = 0$ on the $x - z$ plane, folded as described in Eq. (15) of Ref. [13].
- mission elapsed time, measured relative to January 1, 2001,
- conversion type (front or back), indicates whether the event induced pair production in the front (thin) layers or the back (thick) layers of the tracker,

- the magnetic field in which the LAT is immersed, as parameterized by the McIlwain B and L parameters [15],

III. SPECTRA

For the observed feature we assume a single line where the pdf $f_{\text{line}}(E_\gamma|E_{\text{line}})$ is defined according to the Fermi-LAT energy dispersion tools definition [16] with a true photon energy of E_{line} (see Fig.3 of Ref [9]). To analyze the energy dependence, we integrate out the dependence on θ using the exposure and livetime in the region of interest.

The background pdf is a simple power-law:

$$f_{\text{bg}}(E_\gamma|\beta, \alpha) = \beta \left(\frac{E_\gamma}{E_0} \right)^{-\alpha}$$

A. Earth's Limb Spectrum

Some fraction of the time, the LAT's field of view includes the limb of the Earth, where photons are produced in collisions of cosmic rays with the atmosphere. These are not salient for dark matter searches, given their terrestrial source, and so are typically discarded. The observation of a statistically significant feature near $E_\gamma = 130$ GeV in this spectrum for photons with $30^\circ < \theta < 45^\circ$ (Ref [7] and Fig. 1) where none is expected from dark matter annihilation points strongly to an instrumental explanation of this feature.

B. Solar Spectrum

In the same spirit, we examine the high-energy Solar spectrum. The Fermi collaboration studied the low-energy ($E_\gamma < 10$ GeV) spectrum in a smaller dataset [17].

While arguments have been made that the Sun's gravitational well may trap dark matter particles [18], and searches have been performed for evidence of Solar dark matter annihilation via neutrinos [19], the majority of the dark matter is expected to be gathered near the center of the Sun. Photons resulting from Solar dark-matter annihilation would not escape the Sun without interacting, and so no signal is expected in the Solar photon spectrum[21] unless the Solar dark matter halo is much broader, contrary to current ideas (*e.g* Ref [20]). A feature in the Solar spectrum would suggest instrumental causes, in the same manner as the peak in the Earth's limb data.

To isolate Solar photons, we use the position of the Sun relative to the LAT and calculate the effective position of the Sun in galactic coordinates at the moment a given photon is received, (b_\odot, l_\odot) . The Solar region is then defined via the angular distance

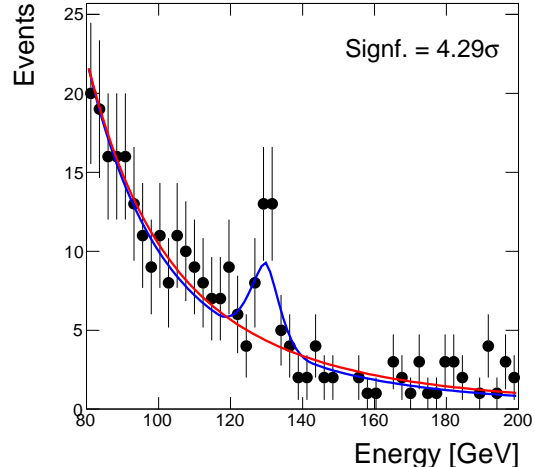


FIG. 1: Observed Fermi-LAT photon spectrum from the Earth's limb, requiring in addition $30^\circ < \theta_{\text{photon}} < 45^\circ$, following Ref. [7].

$$\cos(\Delta R_\odot) = \sin(b_\gamma) \sin(b_\odot) + \cos(b_\gamma) \cos(b_\odot) \cos(l_\gamma - l_\odot)$$

We consider photons with $\Delta R_\odot < 5^\circ$ outside the region of the galactic center (see Fig. 2, left) to be Solar photons. The Solar photon spectrum is shown in Fig. 2 (right), compared to the spectrum of the inverted region ($\Delta R_\odot > 5^\circ$, same veto on galactic center photons). The local statistical significance of the feature near $E_\gamma = 135$ GeV is 3.2σ (see Fig. 4) which does not suffer from a look-elsewhere effect, as the region-of-interest in E_γ of the feature is determined by the feature in the galactic center spectrum. This appears to be the first examination of the high-energy Solar spectrum ($E_\gamma > 10$ GeV) using Fermi-LAT data. The same feature appears for different requirements of ΔR_\odot , see Fig. 3; in fact, masking out the physical extent of the Sun ($\Delta R_\odot \in [1, 5]^\circ$) yields nearly the same spectrum, suggesting that these photons do not originate from the Sun proper, but from its vicinity.

IV. INSTRUMENTAL STUDY WITH SPLOTS

To consider potential instrumental explanations of the observed features, we ask whether the photons in the peaks have distinct instrumental characteristics from the background photons. A naive approach would be to simply divide the photons into two categories by energy range; this leaves the peak-region sample with significant background contamination. A superior technique is statistical unfolding using the sPLOTS algorithm [11].

If a sample of events contains contributions from multiple sources, whose relative contributions can be measured by fitting pdfs in a discriminating variable, the

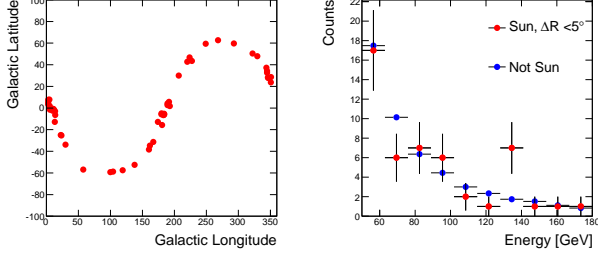


FIG. 2: Left, galactic coordinates of photons within $\Delta R_{\odot} < 5^{\circ}$ of the position of the Sun. Right, energy spectrum for photons from the vicinity of the Sun ($\Delta R_{\odot} < 5^{\circ}$, excluding the galactic center), compared to photons from the rest of the sky ($\Delta R_{\odot} > 5^{\circ}$, excluding the galactic center), normalized to equal yield.

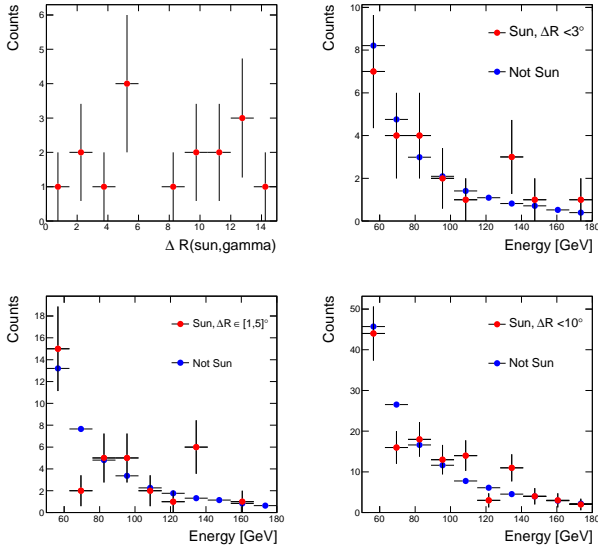


FIG. 3: Clockwise from top left: distribution of ΔR_{\odot} for photons with $E_{\gamma} \in [125, 140]$ GeV; energy spectra for photons from the vicinity of the Sun using $\Delta R_{\odot} < 3^{\circ}$, $\Delta R_{\odot} < 10^{\circ}$, or $\Delta R_{\odot} \in [1, 5]^{\circ}$, excluding the galactic center, compared to photons from the rest of the sky, again excluding the galactic center.

sPLOTS algorithm can statistically extract the distribution of each of the sources in other variables of interest, which we refer to as the ‘unfolding variables’. Note that sPLOTS requires knowledge of the pdf in the discriminating variable, but no assumptions are required of the pdfs in the unfolding variable other than that the pdfs can be factorized between the discriminating and unfolding variables. For a brief derivation of sPLOTS, examples in toy data and application to the Fermi-LAT galactic center spectrum, see Ref [9].

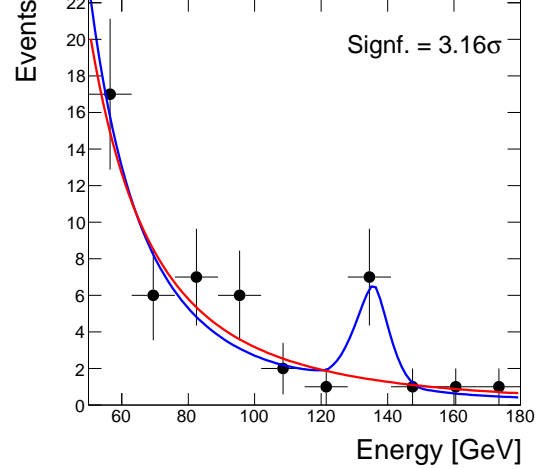


FIG. 4: Energy spectrum as shown in Fig. 2 for photons from the vicinity of the Sun ($\Delta R_{\odot} < 5^{\circ}$), excluding the galactic center, with background-only and background-plus-signal hypotheses.

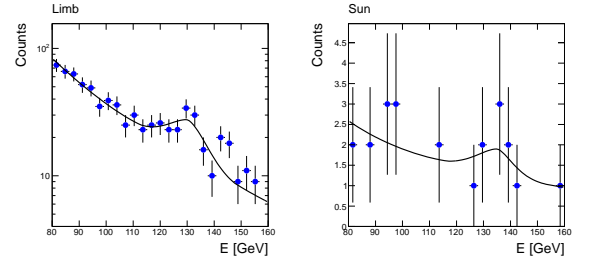


FIG. 5: Energy of Fermi-LAT photons with signal plus background fit. Left is the spectrum from the Earth’s limb with $\theta < 60^{\circ}$, right is the Solar spectrum with $\Delta R_{\odot} < 5^{\circ}$, excluding the galactic center.

A. Analysis

To analyze the features of the Fermi-LAT data using sPLOTS, we must fit the background and signal pdfs described above in the discriminating variable, E_{γ} . Applying these pdfs to the observed limb and Solar photon energy spectrum yields the fits seen in Fig. 5. In the limb spectrum, we have not required $30^{\circ} < \theta < 45^{\circ}$ as is done in Fig. 1, but instead we apply a looser requirement $\theta < 60^{\circ}$ in order to study the θ -dependence.

Unfolded distributions of incidence angles are shown in Fig. 6. The recorded time and conversion type are in Fig. 7. The magnetic field parameters are shown in Fig. 8.

In each case, we compare the distributions quantitatively by calculating the χ^2/dof between the peak and background distributions. As the signal and background weights are anti-correlated, this is calculated as

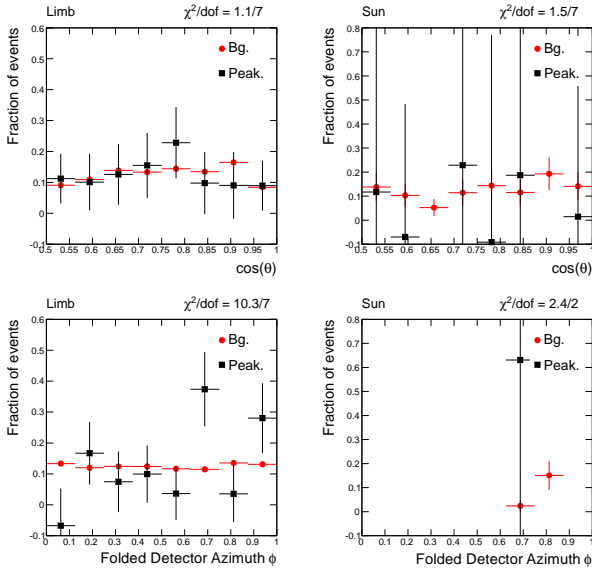


FIG. 6: Disentangled signal and background distributions. Top, $\cos(\theta)$ where θ is the photon incidence angle relative to a line normal the Fermi-LAT face. Bottom, ϕ , the photon incidence angle relative to the sun-facing side [14]. Left are photons from the Earth’s limb, right are photons from the vicinity of the Sun. For the Solar spectrum, ϕ is aligned with respect to Fermi’s solar panels, which track the Sun.

$$\chi^2 = \sum_{\text{bin } i} \frac{(N_{\text{peak}}^i - N_{\text{bg.}}^i)^2}{(\Delta N_{\text{peak}}^i + \Delta N_{\text{bg.}}^i)^2}$$

where N_{peak}^i is the sum of the weights $\sum sP_{\text{peak}}$ in that bin, and ΔN_{peak}^i is calculated from toy simulations which estimate the expected variance of the measurement in each bin. Similar expressions apply for the background uncertainties.

B. Discussion

Our previous analysis of the galactic center feature showed that a large fraction of peak photons had $\cos(\theta)$ near 0.7, unlike the photons from the background (Fig. 5 in Ref. [9]). The limb feature photons also peak near this region, first reported in Ref [7], and confirmed here, see Fig. 6. The Solar spectrum statistics are too poor to contribute to this question.

The galactic center instrumental analysis also showed some discrepancy in the magnetic field environment of the LAT when the photons were recorded (Fig. 11 in Ref. [9]), near 1.6 Gauss. The limb photons have a minor discrepancy near 1.5 Gauss, but entirely consistent with statistical fluctuations. Similarly, the galactic center photons have a feature near folded azimuth $\phi = 0.8$; the limb photons have some features near $\phi = 0.7$ and

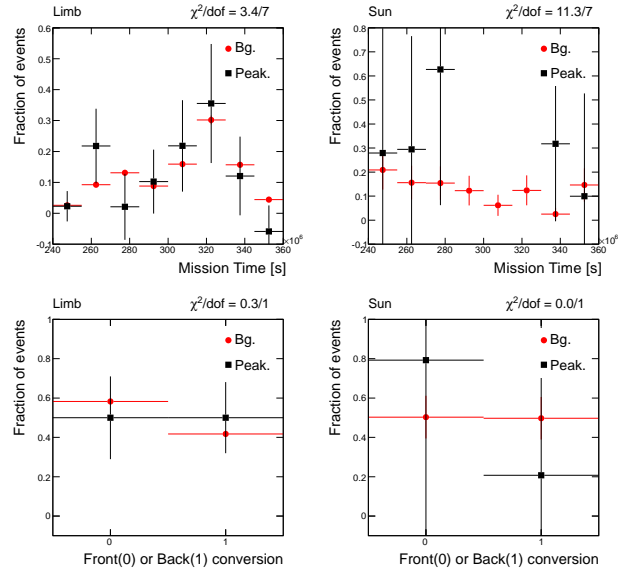


FIG. 7: Disentangled signal and background distributions. Top, the mission elapsed time since Jan 1 2001 [14]. Bottom, fraction of events in which the pair production is induced in the front (thin) or back (thick) layers of the tracker. Left are photons from the Earth’s limb, right are photons from the vicinity of the Sun.

$\phi = 0.9$, but a deficit near $\phi = 0.8$ with respect to the background photons.

V. THE REST OF THE SKY

If the feature near $E_\gamma = 130$ GeV has an instrumental rather than astrophysical explanation, then it should be independent of the source of the photons and one should be able to identify similar features in any spectrum. The full-sky spectrum with no restrictions on instrumental characteristics does not show such a feature; if it exists, a feature in the full-sky spectrum may be localized to particular instrumental regions and washed out in the unrestricted spectrum.

To discover potential instrumental causes, we look for universal characteristics of the peaks found in the three spectra. If the full sky spectrum in a restricted range of these instrumental characteristics were to reveal a feature near $E_\gamma = 130$ GeV, it would lend support to the instrumental explanation.

We first consider the incident angle, θ , already shown to reveal the Earth’s limb peak. In Fig. 9, we show the spectra in the three regions defined earlier: the galactic center, the Sun, and the Earth’s limb. In addition, we show the spectrum in the rest of the sky, defined by requiring zenith angle $< 105^\circ$, rocking angle $< 52^\circ$, $\Delta R_\odot > 5^\circ$, and $\Delta R_{\text{GC}} = \cos^{-1}(\cos(b)\cos(l)) > 5^\circ$. These four regions are disjoint.

First, we examine the spectrum with no restrictions on θ . There are features in the galactic center and Solar

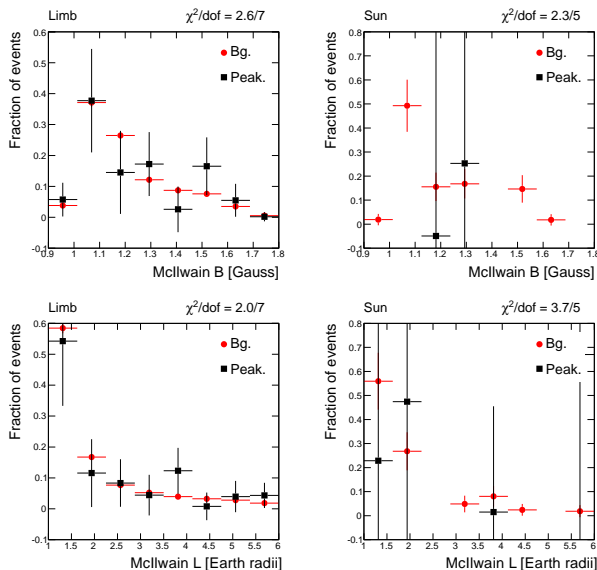


FIG. 8: Disentangled signal and background distributions. Top, magnetic field strength in terms of the McIlwain B parameter. Bottom, the McIlwain L parameter. Left are photons from the Earth’s limb, right are photons from the vicinity of the Sun.

spectrum, but nothing evident in the limb or sky. When we restrict θ to $[30, 45]^\circ$, the limb feature is evident, and we appear to capture a large fraction of the galactic center and Solar features. Most interestingly, a small feature is evident in the sky spectrum near $E_\gamma = 130$ GeV. This feature is intriguing, but is not large enough to unambiguously confirm an instrumental issue in the region θ to $[30, 45]^\circ$.

A similar analysis using the detector azimuth (Fig. 10) is able to capture most of the galactic center, but do not reveal features in the limb or sky spectra.

VI. CONCLUSIONS

We report a spectral feature near $E_\gamma = 130$ GeV in the spectrum of photons from the vicinity of the Sun, where none is expected from dark matter annihilations. The statistical significance is 3.2σ , corresponding to a p -value of $< 0.5\%$ that the feature is a statistical fluctuation. This is the first report of such a feature. Based on current understanding of the Solar dark matter halo, if the feature in the Solar spectrum is more than statistical fluctuation, it represents evidence of instrumental issues, not dark matter annihilation.

We also analyze the instrumental characteristics of the Earth’s limb feature, and attempt to identify a universal characteristic of photons in the three observed features using the SPLOTS algorithm.

Finally, we show that a narrow range of incident photon angles includes many photons from the observed peaks, and reveals a feature near $E_\gamma = 130$ GeV in the

spectrum of the remainder of the sky. While we attempt to remove dependence on photon source by examining the full sky and placing restrictions only on θ , instrumental characteristics may in general be correlated with the photon source, as the geometry of the Sun, Earth and galactic center relative to the LAT may give different average distributions of instrumental characteristics. If the spectral feature were caused by an instrumental issue in a slice of θ and another not-yet-identified variable, it is plausible that photons from the Earth, Sun and galactic center sweep across this slice differently, giving different θ -dependences and explaining the stronger θ -dependence of the limb and sky features than in the solar and galactic center features. In addition, more precisely focusing on photons in such a slice would enhance the feature in the sky spectrum.

While this does not give a definitive instrumental explanation for these spectral features, it casts significant further doubts on the dark matter hypothesis.

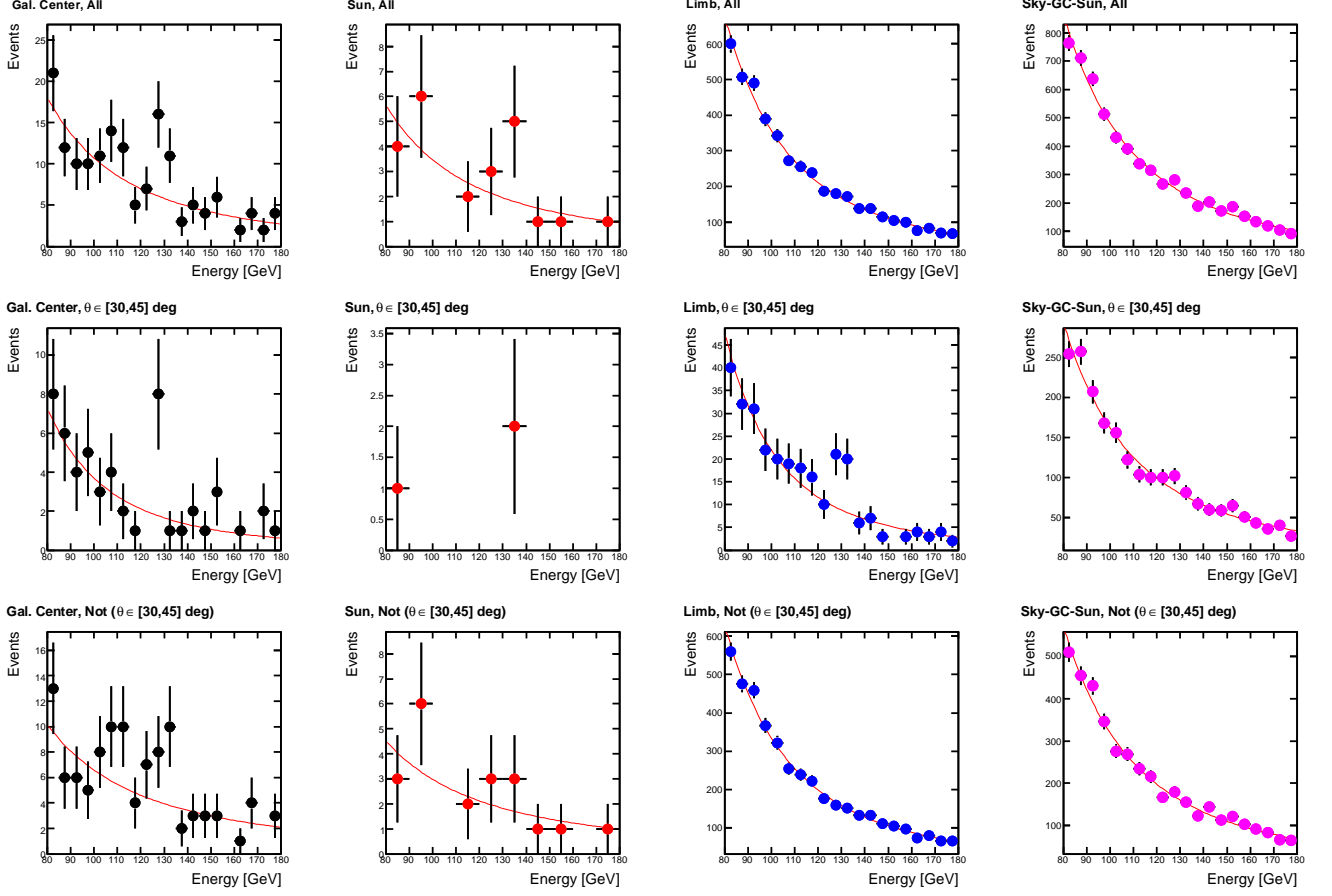


FIG. 9: Energy spectra for four regions; from left: galactic center, Solar vicinity, Earth's limb, and the full sky with the GC and Sun removed. Top shows the complete spectrum, center is for photons with incident angle θ in the range $[30, 45]$ degrees, and bottom for photons with θ out of the range $[30, 45]$ degrees.

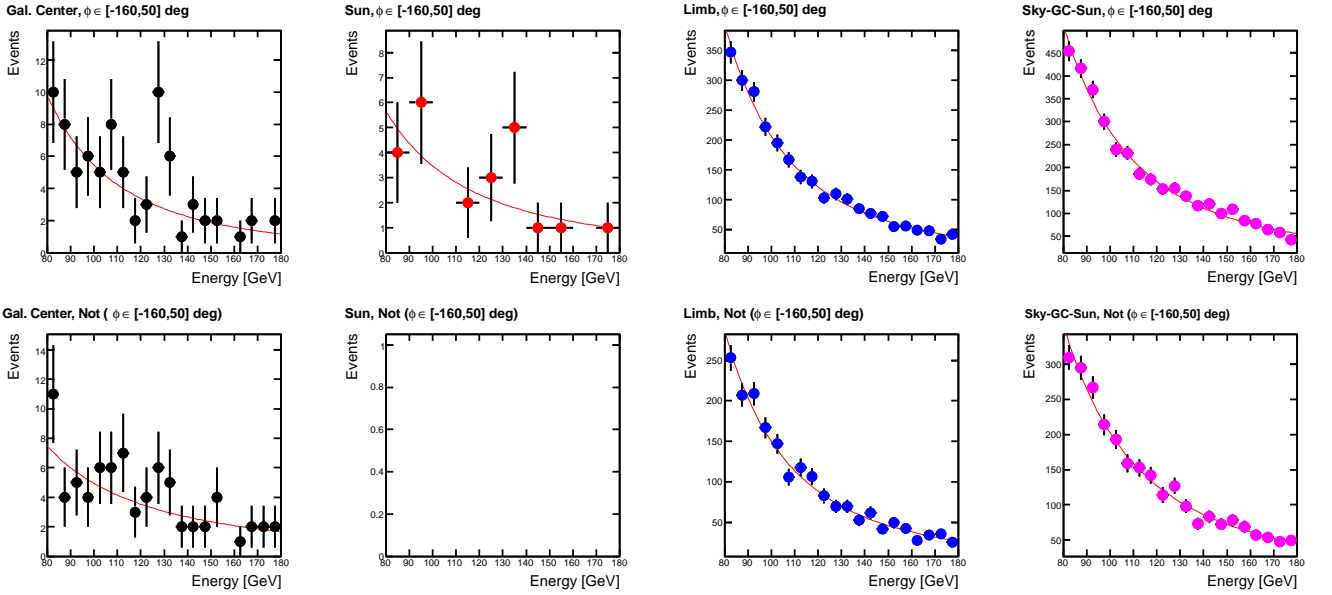


FIG. 10: Energy spectra for four regions; from left: galactic center, Solar vicinity, Earth's limb, and the full sky with the GC and Sun removed. Top is for photons with azimuth angle ϕ in the range $[-160, 50]$ degrees, and bottom for photons with ϕ out of the range $[-160, 50]$ degrees.

Acknowledgments

VII. ACKNOWLEDGEMENTS

DW acknowledges contributions, explanations and useful discussions with Eric Albin which are clearly deserving of authorship, and comments from Itay Yavin, Andrew Nelson, and Kanishka Rao. DW is supported by grants from the Department of Energy Office of Science and by the Alfred P. Sloan Foundation. DW is grateful to the Aspen Center for Physics, where this some of this work was performed and supported by NSF grant no. 1066293.

-
- [1] W. B. Atwood *et al.* [LAT Collaboration], *Astrophys. J.* **697**, 1071 (2009)
 - [2] A. A. Abdo *et al.* [The Fermi-LAT Collaboration], *Phys. Rev. Lett.* **104**, 091302 (2010) [arXiv:1001.4836]
 - [3] M. Ackermann *et al.* [Fermi-LAT Collaboration], (2012), arXiv:1205.2739
 - [4] T. Bringmann, X. Huang, A. Ibarra, S. Vogl and C. Weniger, (2012), arXiv:1203.1312
 - [5] C. Weniger, (2012), arXiv:1204.2797
 - [6] E. Tempel, A. Hektor and M. Raidal, (2012), arXiv:1205.1045
 - [7] M. Su and D. P. Finkbeiner, (2012), arXiv:1206.1616
 - [8] K. Rao and D. Whiteson, arXiv:1210.4934 [astro-ph.HE].
 - [9] D. Whiteson, *JCAP* **1211**, 008 (2012) [arXiv:1208.3677 [astro-ph.HE]].
 - [10] D. P. Finkbeiner, M. Su and C. Weniger, arXiv:1209.4562 [astro-ph.HE].
 - [11] M. Pivk and F. R. Le Diberder, *Nucl. Instrum. Meth. A* **555**, 356 (2005) physics/0402083
 - [12] Pass7, `ultraclean` class, quality requirements: `DATA_QUAL= 1 && LAT_CONFIG=1` and a good time interval (via `gtmktime`).
 - [13] [Fermi-LAT Collaboration], arXiv:1206.1896 [astro-ph.IM].
 - [14] http://fermi.gsfc.nasa.gov/ssc/data/analysis/documentation/Cicerone/Cicerone_Data/LAT_Data_Columns.html
 - [15] McIlwain, C. E., *J. Geophys. Res.* **66**, pp. 3681-3691 (1961).
 - [16] http://fermi.gsfc.nasa.gov/ssc/data/analysis/documentation/Cicerone/Cicerone_LAT_IRFs/IRF_E_dispersion.html
 - [17] A. A. Abdo, M. Ackermann, M. Ajello, L. Baldini, J. Ballet, G. Barbiellini, D. Bastieri and K. Bechtol *et al.*, *Astrophys. J.* **734**, 116 (2011)
 - [18] A. H. G. Peter, arXiv:0905.2456 [astro-ph.HE].
 - [19] R. Abbasi *et al.* [IceCube Collaboration], arXiv:1111.2738 [astro-ph.HE].
 - [20] N. Weiner and I. Yavin, *Phys. Rev. D* **87**, 023523 (2013) [arXiv:1209.1093 [hep-ph]].
 - [21] S. Sivertsson and J. Edsjo, *Phys. Rev. D* **81**, 063502 (2010) [arXiv:0910.0017 [astro-ph.HE]].